

Article

Three-Dimensional Finite Element Modeling of Ultrasonic Vibration-Assisted Milling of the Nomex Honeycomb Structure

Tarik Zarrouk ^{1,2,*} , Mohammed Nouari ^{2,*}, Jamal-Eddine Salhi ^{3,4} , Mohammed Abbadi ⁵  and Ahmed Abbadi ⁵¹ CREHEIO (Centre de Recherche de L'Ecole des Hautes Etudes d'Ingénierie), Oujda 60000, Morocco² CNRS, LEM3, IMT, GIP InSIC, Université de Lorraine, F-88100 Saint Dié des Vosges, France³ Department of Mathematics, Saveetha School of Engineering, SIMATS, Chennai 602105, Tamil Nadu, India; j.salhi@ump.ac.ma⁴ Laboratory of Energetics (LE), Faculty of Sciences, Abdelmalek Essaadi University, Tetouan 93000, Morocco⁵ Laboratory of Mechanics and Scientific Calculation, National School of Applied Sciences, Oujda 60000, Morocco

* Correspondence: zarrouk.tarik@ump.ac.ma (T.Z.); mohammed.nouari@univ-lorraine.fr (M.N.)

Abstract: Machining of Nomex honeycomb composite (NHC) structures is of critical importance in manufacturing parts to the specifications required in the aerospace industry. However, the special characteristics of the Nomex honeycomb structure, including its composite nature and complex geometry, require a specific machining approach to avoid cutting defects and ensure optimal surface quality. To overcome this problem, this research suggests the adoption of RUM technology, which involves the application of ultrasonic vibrations following the axis of revolution of the UCK cutting tool. To achieve this objective, a three-dimensional finite element numerical model of Nomex honeycomb structure machining is developed with the Abaqus/Explicit software, 2017 version. Based on this model, this research examines the impact of vibration amplitude on the machinability of this kind of structure, including cutting force components, stress and strain distribution, and surface quality as well as the size of the chips. In conclusion, the results highlight that the use of ultrasonic vibrations results in an important reduction in the components of the cutting force by up to 42%, improves the quality of the surface, and decreases the size of the chips.

Keywords: modeling finite elements (EF); NHC core; RUM technology; UCK cutting tool; surface quality; stress and strain distribution; chip size



Citation: Zarrouk, T.; Nouari, M.; Salhi, J.-E.; Abbadi, M.; Abbadi, A. Three-Dimensional Finite Element Modeling of Ultrasonic Vibration-Assisted Milling of the Nomex Honeycomb Structure. *Algorithms* **2024**, *17*, 204. <https://doi.org/10.3390/a17050204>

Academic Editors: Sheng Du, Zixin Huang, Li Jin and Xiongbo Wan

Received: 8 April 2024

Revised: 7 May 2024

Accepted: 8 May 2024

Published: 10 May 2024



Copyright: © 2024 by the authors. Licensee MDPI, Basel, Switzerland. This article is an open access article distributed under the terms and conditions of the Creative Commons Attribution (CC BY) license (<https://creativecommons.org/licenses/by/4.0/>).

1. Introduction

The aerospace and aeronautics sectors place significant emphasis on developing solutions that integrate lightweight materials with exceptional performance characteristics, particularly in demanding and extreme environments [1,2]. This pursuit is driven by the need to enhance fuel efficiency, reduce emissions, and improve overall operational efficiency in aircraft and spacecraft applications. Lightweight materials, such as advanced composites including carbon fiber-reinforced polymers and Nomex material, offer substantial weight savings without compromising strength and durability [3,4]. Due to their notable mechanical properties, Nomex honeycomb structures are widely used in these sectors, particularly in the manufacturing of aircraft wings and tails [5,6]. However, shaping these structures presents a challenge due to the geometry of the NHC core and the fragility of the Nomex paper that comprises it [7]. Shaping of the honeycomb structure is usually carried out through conventional processes such as cutting using thin-bladed tools [8]. However, these methods are limited by their efficiency, the presence of significant machining defects, high cutting forces, and rapid tool wear as well as significant dust pollution [9,10]. For this purpose, RUM technology was applied to overcome the problems of conventional cutting of the honeycomb structure. The interest in this new technology is gradually increasing to machine a wide range of conductive and dielectric

materials, including titanium and aluminum alloys [11,12]. For example, Xia et al. [13] conducted a study to optimize the dimensions of an ultrasonic disc tool with the aim of evaluating the influence of its geometric properties on its energy density and stiffness. Their results demonstrated a significant correlation between the processing efficiency of the NHC structure and geometric parameters such as cutting angle. The study carried out by Sun et al. [14] shows the benefits of integrating rotary ultrasonic machining (RUM) into the milling process of aluminum honeycomb structures. Their study established that the use of this technology resulted in the reduction of the cutting force, which helped to mitigate the plastic deformation of the walls of the structure. In general, the machining of Nomex honeycomb structures is often carried out using an experimental approach, with direct involvement of the machine tool. In this regard, Ahmad et al. [15] compared the cutting forces generated during the milling of Nomex honeycomb composites (NHCs), using conventional and ultrasonic machining. Their results demonstrated that ultrasonic vibration machining induced a notable reduction in cutting forces. In the same way, Kang et al. [16] carried out a comparative study of the quality machined surface of the Nomex honeycomb structure using rotary ultrasonic milling (RUM) technology and conventional milling. Their findings demonstrated a notable reduction in the formation of defects on surfaces generated by ultrasonic vibration-assisted machining. In this perspective, Xiang et al. [17] proposed the use of a disc milling cutter with vibration conditions combining longitudinal torsion for the machining of Nomex honeycomb composites (NHCs). Their research found that adding torsional vibrations to longitudinal vibrations not only increased the instantaneous cutting speed of the cutting disc but also promoted material breakage. These improvements result in shorter burrs, reduced burr rates, and less tearing. Due to the rapid movement of the cutting tool and the difficulty in accessing the interface between the cutting tool and the structure to be machined, the experimental process fails to adequately follow the cutting process and the formation of shavings. Therefore, numerical modeling presents itself as a valuable tool for monitoring chip formation and analyzing in detail the machinability characteristics of the structure. Nevertheless, the significant lack of numerical work detailing the machining process of Nomex honeycomb structures highlights the growing imperative to conduct research based on numerical simulations in order to better understand and optimize the machining of these particular structures. In this direction, Wojciechowski et al. [18] proposed a comprehensive micro-milling cutting force model, highlighting high accuracy in predicting forces during the cutting operation. Furthermore, Yuan et al. [19] developed an accurate mechanistic model of cutting force specific to micro-end milling, demonstrating the agreement between the developed numerical model and experimental results. This paper presents a 3D numerical model FE for ultrasonic vibration-assisted milling of the Nomex honeycomb core, developed using the commercial software ABAQUS. From this model, various aspects were carefully examined to optimize the machinability of this type of structure. In conclusion, the results highlight that the application of ultrasonic vibration results in a notable decrease in the cutting force components, while improving the machined surface and reducing the chip size.

2. Finite Element Model

2.1. Material Parameters

Experimental research has focused on exploring the milling characteristics of Nomex honeycomb composite (NHC) structures using the THU Ultrasonic 850 machine tool, which was developed by Tsinghua University in China (refer to Figure 1) [20]. This specialized machine tool incorporates ultrasonic vibration technology to enhance machining efficiency and precision when working with composite materials like Nomex honeycomb. By utilizing the THU Ultrasonic 850, researchers can investigate and optimize milling parameters such as feed rate, spindle speed, and vibration amplitude to achieve the desired machining outcomes. This experimental approach not only advances the understanding of NHC machining processes but also contributes to the development of innovative manufacturing techniques for aerospace and other high-performance applications. In order to validate

the obtained results of the experiment, a numerical approach using the finite element (FE) method is proposed. In the context of machining simulation, it is essential to precisely establish the geometric characteristics of the part and the cutting tool. This approach is crucial to guarantee the accuracy and reliability of the results, which makes it imperative to carefully define the mechanical properties of the structure as well as the cutting tool. The materials forming the Nomex honeycomb structure are composed of aramid fibers and phenolic resin, recognized for their high mechanical and thermal resistance. The geometric characteristics of the cell are shown in Figure 1.

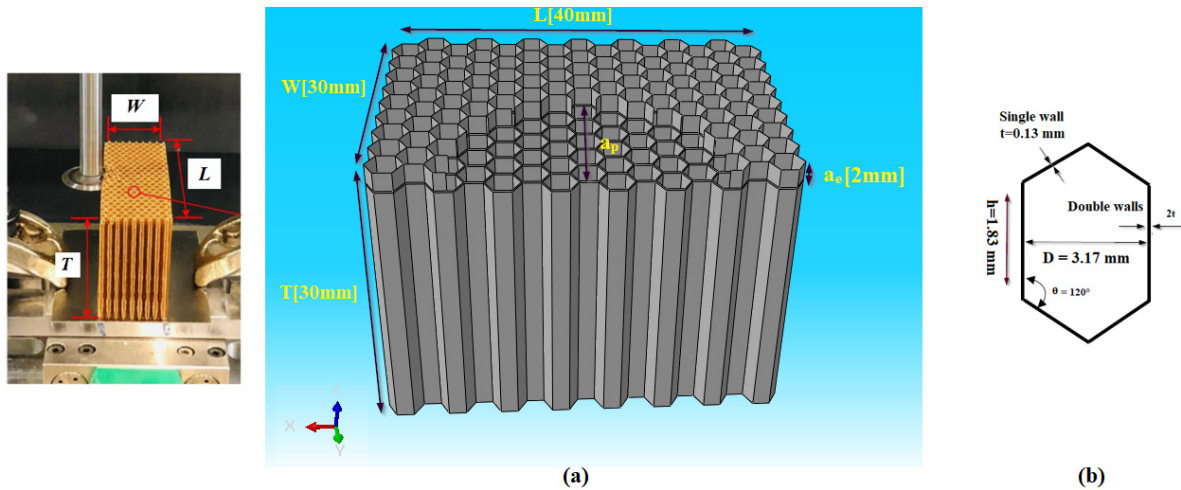


Figure 1. (a) Dimensions of the Nomex honeycomb structure (NHC); (b) Dimensions of the alveolar cell [21].

In accordance with the experimental methodology, milling was conducted using a specific cutting tool designated as a high-speed steel (HSS-W18Cr4V) ultrasonic circular milling cutter (See Figure 2) [20]. For this purpose, the design of the UCK tool was designed, considering the geometric parameters used throughout the experimental step (See Figure 3).

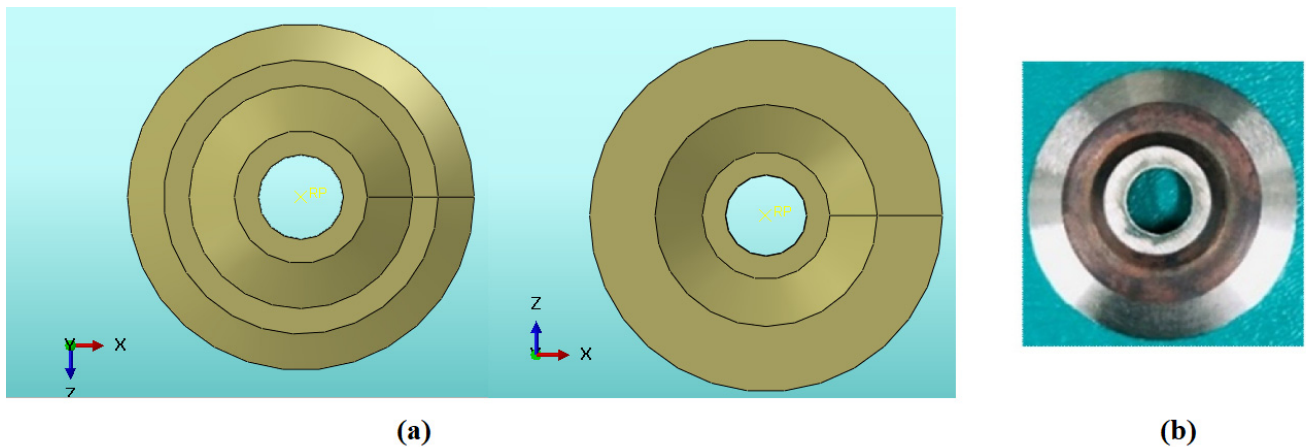


Figure 2. UCK cutting tool: (a) UCK used in milling simulation; (b) UCK used in the experiment phase.

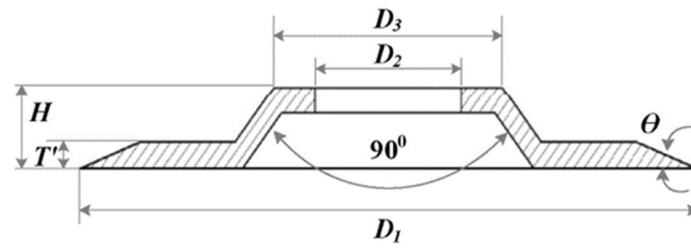


Figure 3. Dimensions of the UCK milling cutter.

2.2. Law of Behavior Applied

Milling of a composite structure requires subjecting the material to significant deformation when in contact with a cutting tool, which results in the creation of chips. Thus, it is essential to determine the constitutive law appropriate to the material constituting the part and the cutting tool in order to be able to carry out effective numerical simulations. In this work, the material constituting the NHC core exhibits isotropic elastoplastic behavior [22,23]. This behavior is made up of two parts: a reversible elastic part and an irreversible plastic part, as described in Equation (1).

$$\epsilon = \epsilon^{el} + \epsilon^p \tag{1}$$

ϵ is the total stress tensor, and ϵ^{el} and ϵ^p represent the elastic and plastic strain tensor, respectively.

In general, the elastic behavior of the material is described using Hooke’s law, which constitutes a fundamental model of linear elasticity. This law describes a linear relationship between the stress σ and the strain ϵ of elastic materials according to Equation (2).

$$\{\epsilon\} = [C] \{\sigma\} \tag{2}$$

C is the tensor of the reasoner of order 4.

The law, therefore, becomes the following:

$$\begin{pmatrix} \epsilon_{11} \\ \epsilon_{22} \\ \epsilon_{33} \\ \epsilon_{23} \\ \epsilon_{31} \\ \epsilon_{12} \end{pmatrix} = \begin{pmatrix} \frac{1}{E} & -\frac{\nu}{E} & -\frac{\nu}{E} & 0 & 0 & 0 \\ -\frac{\nu}{E} & \frac{1}{E} & -\frac{\nu}{E} & 0 & 0 & 0 \\ -\frac{\nu}{E} & -\frac{\nu}{E} & \frac{1}{E} & 0 & 0 & 0 \\ 0 & 0 & 0 & \frac{1}{G} & 0 & 0 \\ 0 & 0 & 0 & 0 & \frac{1}{G} & 0 \\ 0 & 0 & 0 & 0 & 0 & \frac{1}{G} \end{pmatrix} \begin{pmatrix} \sigma_{11} \\ \sigma_{22} \\ \sigma_{33} \\ \sigma_{23} \\ \sigma_{31} \\ \sigma_{12} \end{pmatrix} \tag{3}$$

To precisely define the elastic properties of a material, it is essential to determine the Lamé coefficients, λ and μ . These coefficients are linked to Young’s modulus E and Poisson’s ratio ν by Equations (4) and (5).

$$\lambda = \frac{\nu E}{(1 + \nu)(1 - 2\nu)} \tag{4}$$

$$\mu = \frac{E}{2(1 + \nu)} \tag{5}$$

Isotropic elastoplastic behavior has been attributed to Nomex material by several authors [24]. Figure 4 demonstrates the mechanical properties of the Nomex material, highlighting the elastic thresholds and variations in plastic behavior as a function of wall thickness. The principal mechanical characteristics attributed to Nomex material are described in Table 1.

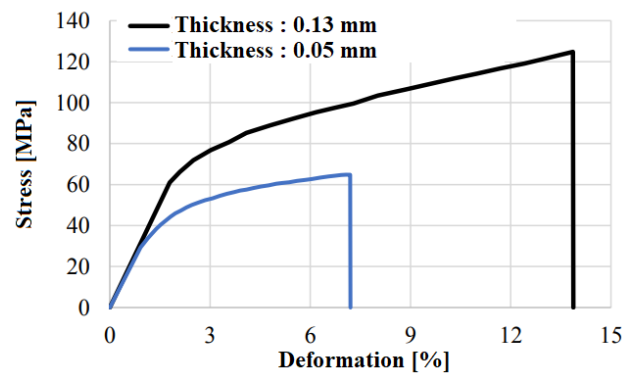


Figure 4. Evolution of the stress and deformation of the Nomex material [22,23].

Table 1. The mechanical properties of Nomex paper [22,23].

Mechanical Properties	
Density [g/cm ³]	1.4
E [MPa]	3400
Poisson's ratio	0.3
Yield strengths for simple wall thickness (MPa)	29
Yield strengths for double wall thickness (MPa)	61

2.3. Chip Separation Criterion

In the machining process, where the material is cut using a suitable cutting tool, defining a failure criterion is of crucial importance to simulate the machining precisely. Failure criteria are usually associated with the intrinsic mechanical and thermal properties of the material. As part of this study, the shear failure criterion is specifically chosen, and its modeling is assigned to the finite element analysis software Abaqus. The process of assessing damage starts with gathering the initial mechanical characteristics, which are detailed in Table 1. Subsequently, the motion of the milling cutter induces a force exerted on the workpiece, where the determination of dynamic normal and shear stresses is carried out through various interfaces. When the rupture coefficient, denoted ω , exceeds a critical threshold of 1 (Equation (6)), it indicates deterioration of the material and the formation of chips.

$$\omega = \sum \frac{\Delta \varepsilon}{\varepsilon^f} \quad (6)$$

where ω represents the shaping limit value or destruction coefficient, $\Delta \varepsilon$ represents the incremental equivalent plastic strain, and ε^f indicates the total strain at which the material experiences damage.

2.4. Finite Element Modeling

This paper provides a simulation study of the rotary ultrasonic machining (RUM)-assisted cutting process of the NHC core. This simulation is based on a numerical FE model developed with the Abaqus/Explicit software. The cell walls of the Nomex honeycomb structure are composed of two-thirds single-cell walls and one-third double-cell walls. The corresponding thicknesses of single- and double-cell walls are set to 0.13 mm and 0.26 mm, respectively, in the numerical model. In this approach, the meshing of the NHC core walls is achieved using reduced-integration four-node S4R shell elements, as shown in Figure 5a. Throughout the numerical modeling, the UCK tool is supposed to be rigid, which means that it is non-deformable during the milling process. Therefore, the UCK milling cutter is meshed using rigid quadrangular elements with four nodes (R3D4), as presented in Figure 5b.

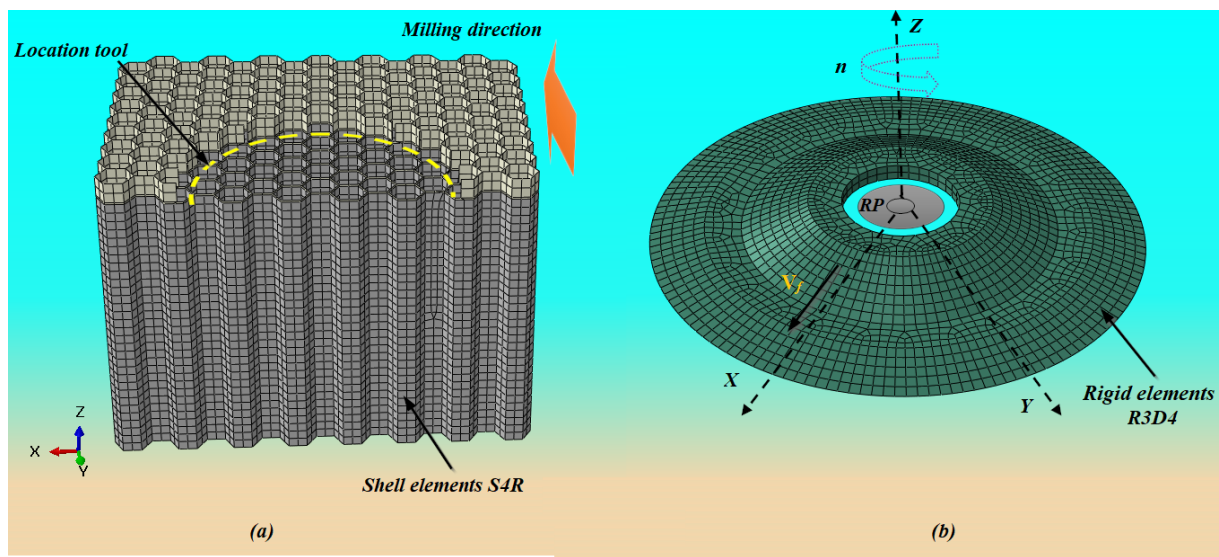


Figure 5. (a) Mesh of the part (NHC); (b) Mesh of the cutting tool and location of reference point (RP) [21].

Before starting the implementation of the numerical code, it is essential to conduct a preliminary phase aimed at examining the nonlinear parameters that can impact the convergence of the numerical results, in particular the type and size of the mesh. It is important to note that using a fine mesh size can result in a substantial increase in calculation time, particularly in the context of 3D configurations. It is, therefore, essential to find an optimal balance between the size of the mesh and the exactness of the results, while maintaining a reasonable calculation time. As part of the simulation of the machining process, a general contact was used to describe the interaction between the UCK milling cutter and the Nomex honeycomb core. Since the walls of the Nomex honeycomb structure are thin, the contact between it and the cutting tool is considered punctual. For this purpose, the friction coefficient adopted to carry out the numerical simulations is set at 0.1. In order to ensure permanent contact between the milling cutter and the workpiece, an initial integration between the part and the tool was set up, taking into account the geometric particularities of the NHC core and the UCK milling cutter (see Figure 5a). The boundary conditions were adopted according to the experimental process [20] so that the lower surface of the NHC structure remained stationary and incapable of undergoing displacements or rotations. For this purpose, in the numerical modeling, complete fixation is imposed on the bottom surface of the NHC core, preventing any translational movement ($U_x = U_y = U_z = 0$) along the X, Y, and Z axes as well as any rotation around these axes ($U_{Rx} = U_{Ry} = U_{Rz} = 0$), as shown in Figure 6b. The difference between conventional milling and ultrasonic vibration-assisted axial milling is the introduction of ultrasonic vibrations along the Z axis at the end of the milling cutter. The ultrasonic rotary machining (RUM) process represents an approach in mechanical manufacturing that involves the synchronization of three types of motions. These motions include translation of the tool along the axis OY, characterized by the feed rate V_f , rotation of the cutting tool around the axis OZ, expressed by the spindle speed n , and the vibration of the tool along the OZ axis, generating a sinusoidal ultrasonic wave (see Figure 6). To guarantee precise monitoring of the milling simulation process, a reference point denoted RP, was assigned along the axis of revolution of the cutting tool in accordance with the representation in Figure 5b. This point assumes an essential role in assigning cutting parameters and in assessing the cutting forces acting throughout the milling operation. In order to describe the motion of the cutting tool, the following equations are used to define its global coordinates xyz :

$$V_x = V_c \cos\left(\frac{2\pi n t}{60}\right) + V_f \tag{7}$$

$$V_y = V_c \sin\left(\frac{2\pi n t}{60}\right) \tag{8}$$

$$V_z = A \sin(2\pi f t) \tag{9}$$

In the current article, A denotes the amplitude of ultrasonic vibration; V_c stands for the cutting speed; and f denotes the vibration frequency, which is fixed at 21.26 KHz.

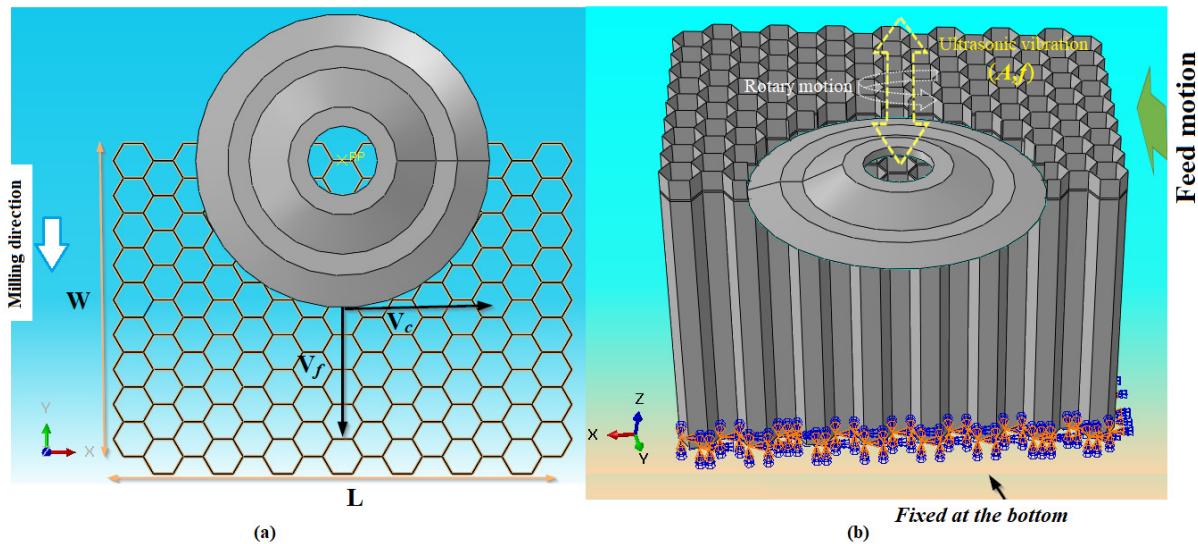


Figure 6. (a) Milling planar representation of the NHC core; (b) Boundary conditions adopted in the numerical modeling [21].

2.5. Components of the Cutting Force

Throughout the experimental stage, the components of the cutting force, denoted by F_y and F_x , are evaluated using the KISTLER-9256C2 dynamometer. The advantage of this technique lies in its ability to determine the average values in both directions using these formulas:

$$F_x = \frac{1}{t_2 - t_1} \int_{t_1}^{t_2} |F_{Cx}| dt \tag{10}$$

$$F_y = \frac{1}{t_2 - t_1} \int_{t_1}^{t_2} |F_{Cy}| dt \tag{11}$$

F_x and F_y represent the average values of the cutting force components along the X and Y axes.

3. Results and Discussion

3.1. Mesh Size Study

The choice of mesh size is closely linked to the nature of the underlying mechanic phenomenon and the objectives of the simulation. This mainly results from its direct effectiveness both on the precision of the results and on the time necessary to carry out the calculation. Although the use of a coarse mesh makes it possible to reduce the calculation time, it results in lower precision of the results. On the contrary, using a finer mesh results in an increase in calculation time, but allows for better-quality results. Thus, during each simulation, it is essential to seek the right accommodation between the size of the mesh, the calculation time, and the precision of the obtained results. In this section, our attention was focused on the impact of mesh size on the components of the cutting force when modeling the milling process. To this end, eight simulations were carried out by adjusting the mesh dimensions, varying from 0.2 mm to 0.9 mm. The simulations were carried out

with the same cutting conditions, including a feed rate of 3000 mm/min, a spindle speed of 5000 rpm, and an amplitude vibration is 25 μm . The obtained results are shown in Figure 7.

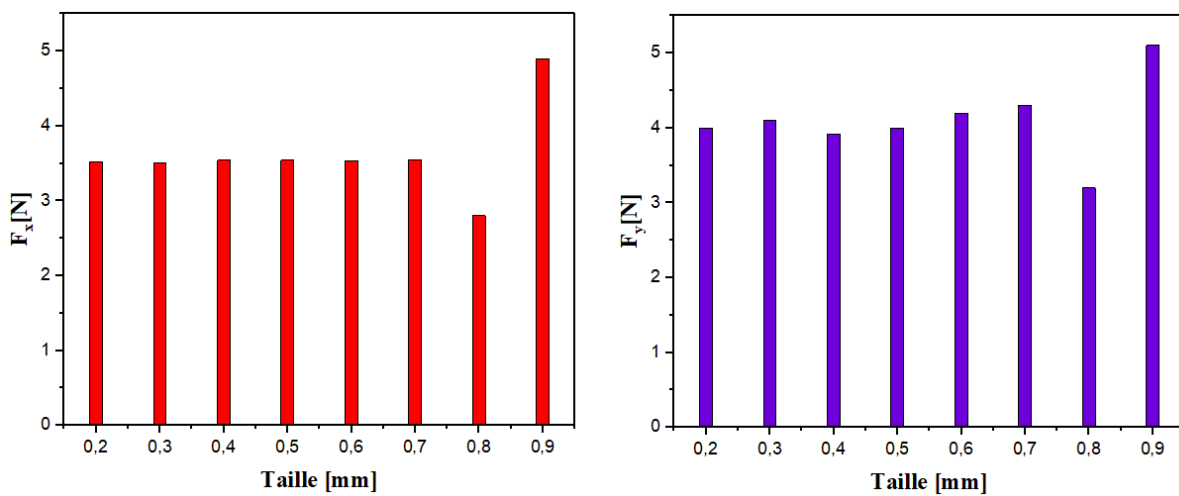


Figure 7. Evolution of the F_x and F_y components as a function of the mesh size.

The convergence range of the mesh is remarkably established between 0.2 mm and 0.6 mm; this observation remains consistent for the two components F_x and F_y . However, the cutting force components recorded a weak decrease between sizes 0.7 mm and 0.8 mm, followed by a sharp increase between sizes 0.8 mm and 0.9 mm. The noticed variation can be credited to the elastic-restoring forces of the NHC core walls. Thus, as soon as the element reaches its breaking point, it is deleted, which results in a loss of contact between the wall of the structure and the milling cutter, leading to a reduction in the F_x and F_y components. Effectively, the force resulting from spring back due to the uncut walls resists the rotation of the tool, thereby increasing the cutting force components. Despite this, small elements have a lower capacity to resist deformation. Therefore, mesh distortion issues manifest themselves more quickly, which can lead to calculation failures. In principle, a mesh size of 0.2 mm seems to provide an ideal compromise between the accuracy of the results and the efficiency of the calculation. However, it was essential to re-evaluate this approach and adapt it to a size of 0.4 mm in order to achieve the best balance between mesh quality and the calculation time. The objective of this adaptation is to guarantee an appropriate resolution of physical phenomena while preventing the deformation of the elements.

3.2. Influence of Cutting Width on Cutting Force Components

A numerical simulation was carried out to verify the validity of the numerical model, evaluating the impact of different cutting widths on the F_x and F_y components when milling the NHC core. This analysis was performed using RUM technology regardless of whether or not ultrasonic vibrations were applied. To carry out this study, four cutting width values were examined, including 4 mm, 6 mm, 8 mm, and 10 mm. Other cutting parameters remained constant throughout the analysis, including a feed rate of 2000 mm/min, a spindle speed of 3000 rpm, and an amplitude vibration is 25 μm . The obtained results are illustrated in Figure 8 [20].

The results of the numerical simulation confirm the experimental tendency noticed for the F_x and F_y components, revealing a significant increase in these components as a function of the cutting width when milling the NHC structure, regardless of whether ultrasonic vibrations are used or not. Increasing the cutting width causes a distension of the contact surface between the milling cutter and the part, which results in an increase in the volume of material removed per unit of time. Similarly, a large cutting width can result in high friction resistance during the machining process, thereby causing an increase in

cutting force components. During the process of cutting the Nomex honeycomb structure using rotary ultrasonic machining, it is clear that the use of ultrasonic vibrations results in a remarkable decrease in the F_x and F_y components, with a reduction reaching up to 42%. In this context, the cutting tool undergoes intense rotation and vibrations, which encourage the formation of cracks in the walls of the NHC structure. This eases the penetration of the tool without encountering resistance from the material constituting the NHC structure. Although increasing the cutting width can improve cutting efficiency, it is also linked to an increase in cutting force components, which can lead to other complications such as premature wear of the cutting tool and degradation of the quality of the machined surface. It is important to determine an optimal value of the cutting width in order to reconcile these two characteristics when machining the NHC core. This optimal value aims to maximize the material removal volume while keeping the cutting force components at a satisfactory level. Thus, this approach guarantees acceptable cutting efficiency and robust numerical results.

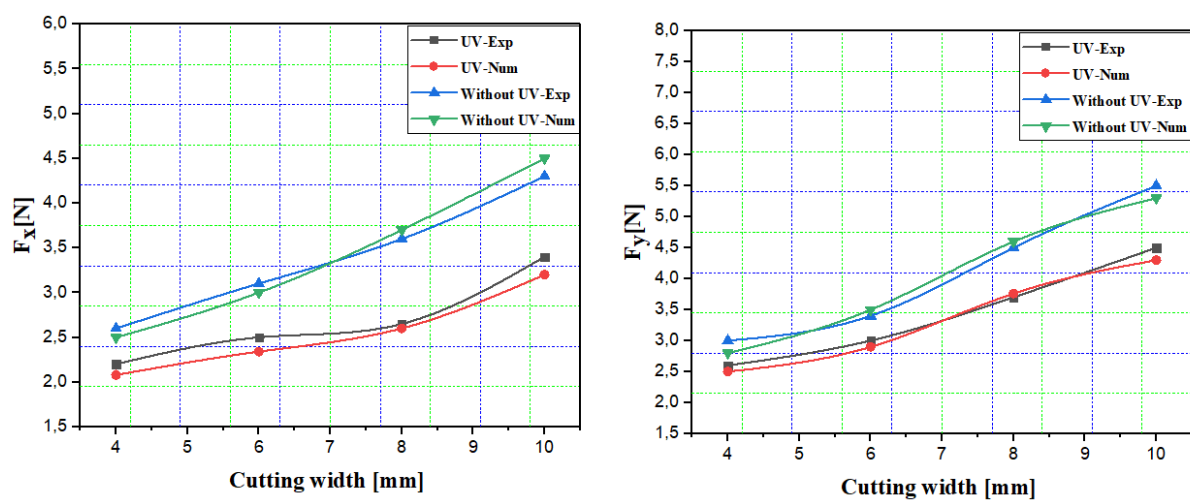


Figure 8. Evolutions of the cutting force components (F_x , F_y).

3.3. Impact of Vibration Amplitude on Machined Surface

The machined surface of the Nomex honeycomb core is essential to building the sandwich structures. Its precise optimization is essential to ensure the robustness and durability of these materials in various industrial applications. Typically, imperfections in the machining of NHC structures come in various forms, including burrs, tears of the walls, and uncut fibers. These defects can appear at different stages of the machining process and have the potential to impact the final quality of the structure. Therefore, in-depth analysis is required to adjust manufacturing parameters and minimize these imperfections. To study the effect of vibration amplitude on the machined surface, numerical simulations were conducted by adjusting the vibration amplitudes to values of 0 μm , 10 μm , and 25 μm . The cutting simulation is carried out under the same cutting conditions, notably a feed rate at 3000 mm/min and a spindle speed at 1000 rpm, which were kept constant throughout the milling simulation. The machining defects generated by the numerical model were spotted by visual inspection with the naked eye and are illustrated in Figure 9.

The main results of this research indicate a gradual enhancement in the quality of the surface with increasing ultrasonic vibration amplitude. This observation highlights a direct relationship between vibration amplitude and surface quality, demonstrating the potential benefits of this technique in machining processes. Furthermore, the numerical results demonstrate that the predominant machining imperfections noticed on the Nomex honeycomb core are wall deformations and tears. Though, the numerical model failed to detect the burrs, characterized by excess material on the cell walls since they were characterized by S4R shell elements without thickness. In fact, at low spindle speeds, the

cutting tool cannot apply adequate force to the walls of the NHC core, which increases the risk of elastic deformation of these walls until their rupture. The use of ultrasonic vibrations highlights the notable benefits they bring to the machining. These vibrations reduce contact between the tool and the thin walls of the honeycomb structure, thereby reducing friction and improving heat dissipation during cutting. The interaction of these parameters facilitates the engagement of the milling cutter with the walls of the honeycomb core, which contributes to the reduction of machining defects and the improvement of the fineness of the machined surface. This finding highlights the effectiveness of ultrasonic vibrations in improving the quality of the machined surface, which allows for improved milling techniques.

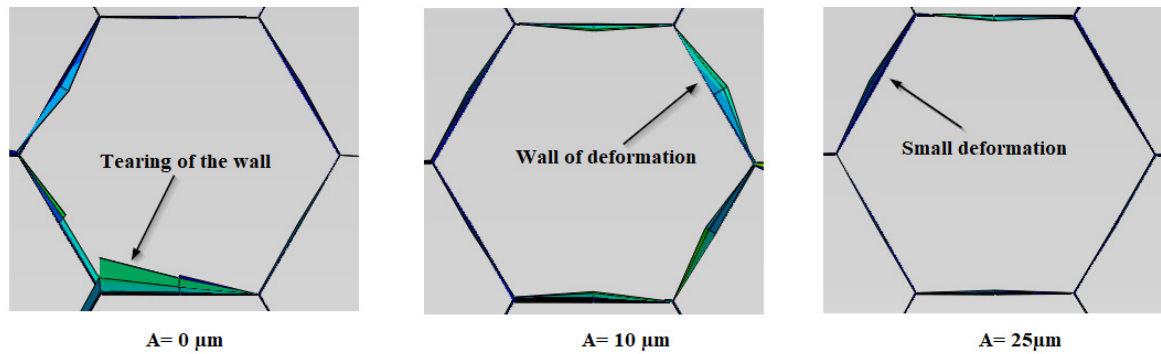


Figure 9. Evolution of the machined surface as a function of the vibration amplitude.

3.4. Analysis of the Distribution of Stresses and Displacements in the Cutting Zone

Studying the stress distribution on the walls of the honeycomb structure of the NHC provides crucial insights into the cutting conditions in the vicinity of the machining zone. This analysis enables a deeper understanding of how ultrasonic vibrations affect the cutting process. By examining the stress patterns, researchers can gain valuable information about how vibrations impact material behavior and chip formation during machining. This enhanced understanding ultimately contributes to optimizing cutting parameters and improving the efficiency and quality of the machining process. This section presents a series of numerical simulations that aim to study the impact of the vibration amplitude on the distribution of stresses and displacements throughout the cutting process of the NHC structure. The vibration amplitudes of the milling cutter were varied at 0 μm, 10 μm, and 25 μm. The simulations are carried out under the cutting parameters, namely a feed rate of 3000 mm/min and a spindle speed of 3000 rpm. The results of these simulations are presented in Figures 10 and 11.

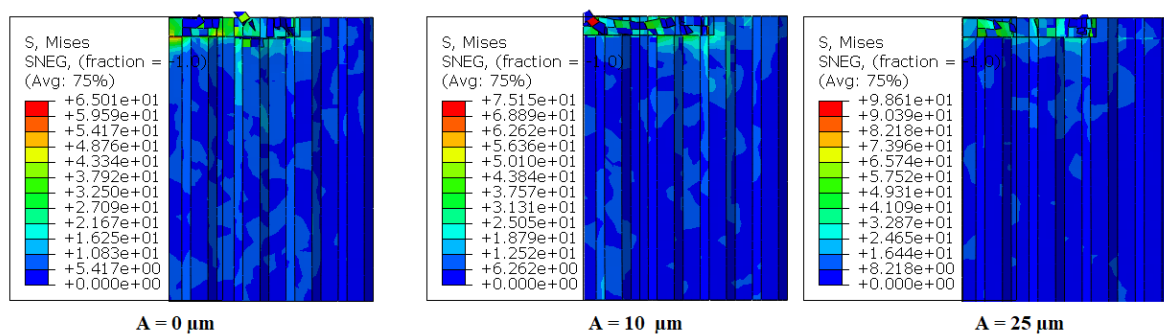


Figure 10. Stress distribution at different vibration amplitudes.

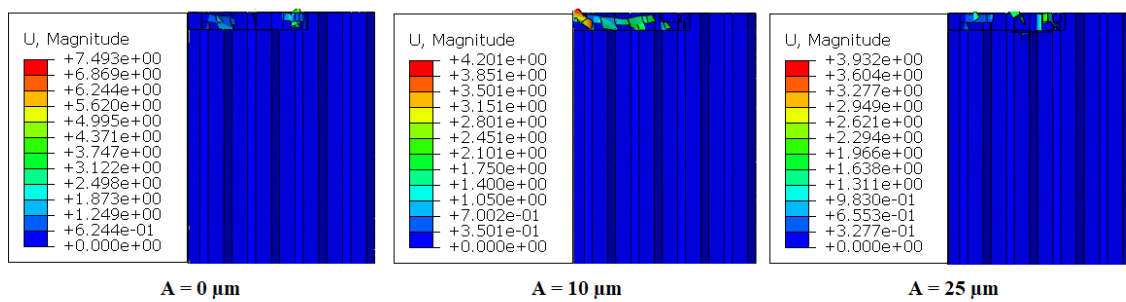


Figure 11. Displacement distribution at different vibration amplitudes.

The study of the stress distribution on the walls of the honeycomb structure of the NHC offers important data on the cutting conditions near the machining zone, which allows a better understanding of the effects of ultrasound vibrations throughout the cutting process. The figures above show the evolution of stresses and displacements of the cell walls for diverse amplitudes. In order to optimize the visual clarity of cell wall stresses and deformations, the representations shown do not include the cutting tool. The rupture occurred under the impact of tall amplitudes, due to the high stresses to reach the established rupture criterion. Elements subjected to stresses below the breaking limit are discernible, while those subjected to higher stresses have suffered fragmentation and are no longer visible. For an amplitude of $0 \mu\text{m}$ (conventional cut), the extreme stress on the structure is evaluated at 65.01 MPa , which is lower compared to the values observed for amplitudes of $10 \mu\text{m}$ and $25 \mu\text{m}$. Nevertheless, the cell wall displacement is meaningfully higher than that seen throughout the ultrasonic cutting process. Therefore, in the ultrasonic cutting process of the Nomex honeycomb, increasing the ultrasound amplitude results in reaching the ultimate strength of the cut cell wall faster, which allows cutting without significant deformations or major damage. In this context, research carried out on ultrasonic vibration-assisted cutting, both for aluminum honeycomb structures, has reached similar conclusions [14,25]. This study demonstrated that the use of ultrasonic vibrations in the cutting process shows consistent results, demonstrating the efficiency and advantages of this method in various situations.

3.5. The Influence of Vibration Amplitude on the Size of the Chips Generated

This section proposes a series of numerical simulations aimed at analyzing the effect of machining techniques on the size of the chips generated. To do this, two techniques were examined: conventional machining without vibrations (amplitude of $0 \mu\text{m}$) and machining assisted by ultrasonic vibrations (amplitude of $15 \mu\text{m}$). It is important to note that the numerical simulations are carried out under the same cutting parameters, namely a feed of 3000 mm/min and a spindle speed of 5000 rpm . The results of this study are presented in Figure 12.

The machining of NHC structures involves a complex two-stage process. Initially, the milling cutter engages with the thin walls of the structure, directing them towards the upper part of the tool where the high spindle speed shreds and pushes the material back, forming chips. This dynamic interaction between the material's structural geometry and the cutting tool is significantly influenced by the rapid spindle rotation, showcasing the intricate responsiveness of machining operations to tool movement and speed. The obtained results demonstrate a clear correlation between chip size and vibration amplitude. Increasing the vibration amplitude leads to a noticeable reduction in chip size, attributed to the combined effect of high-intensity vibrations and rapid spindle speed, which minimizes contact between the milling cutter and the NHC core walls. In this regard, the reduced contact facilitated by high-intensity vibrations and rapid spindle speed allows for easier tool penetration, promoting crack propagation and small chip formation. This reduction in chip size not only lowers cutting forces but also improves overall milling quality and efficiency, extending the cutting tool lifespan.

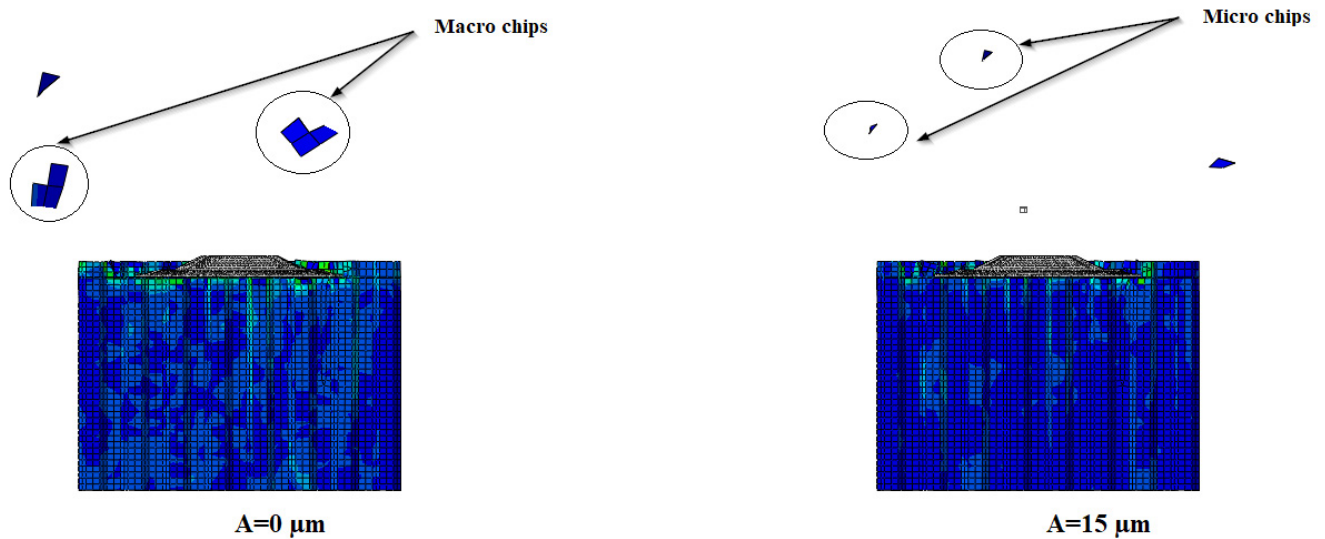


Figure 12. Chip size for different vibration amplitudes.

4. Conclusions

This paper introduces a numerical finite element (FE) model for ultrasonic vibration-assisted milling of Nomex honeycomb structures. Initially, an optimal mesh size was selected to balance CPU calculation time and result accuracy. Simulations were carried out after the validation of the numerical model to analyze the effect of the vibration amplitude on several parameters, notably the quality of the surface, the size of the chips, and the distribution of stresses and displacement in proximity to the cutting zone. Based on this study, the following conclusions can be made:

- The study of the impact of the cutting width on the components of the cutting force is carried out, finding a significant increase in these components with increasing cutting width, both in simulations and in experiments. Our results suggest that the use of ultrasonic vibrations helps to mitigate the negative effects of the F_x and F_y components in both directions. Furthermore, a significant agreement between the results of the numerical model and the experimental data was observed.
- The amplitude of the ultrasonic vibration directly impacts the chip size, leading to a reduction in this one with increasing vibration amplitude.
- The amplitude of the vibration influences the surface quality, leading to an improvement of the latter when the amplitude of the vibrations is increased.
- Applying ultrasonic vibration to the cutting tool induces additional stress in the cutting area of the honeycomb cell wall, accelerating material deterioration while reducing cell wall deformation, facilitating a more efficient milling of the Nomex honeycomb core.
- By continuing this research, it is planned to develop the numerical model by taking into account other parameters in order to detect the burrs that form on the thin walls during the machining process.
- In the industrial context, the optimization of manufacturing processes often requires costly and time-consuming tests to evaluate different configurations. The 3D modeling presented thus offers a considerable advantage in terms of speed, efficiency, and profitability.

Author Contributions: T.Z. performed analyzed and interpreted data and results. M.N. analyzed and interpreted data and was a major contributor to writing the manuscript. J.-E.S. was a major contributor to writing the manuscript. M.A. analyzed and interpreted data and results. A.A. was a major contributor to writing the manuscript. All authors have read and agreed to the published version of the manuscript.

Funding: This research received no external funding.

Data Availability Statement: Data are contained within the article.

Conflicts of Interest: The authors declare no conflicts of interest.

References

1. Zhao, Y.Z.; Yao, S.J.; Xiong, S.W.; Li, B.Y.; Wang, X.Y.; Yang, F.H.; Jia, Y.B.; Wang, L.X.; Wang, H. Preparation of high breakdown strength meta-aramid composite paper reinforced by polyphenylene sulfide superfine fiber. *Polym. Eng. Sci.* **2023**, *63*, 1579–1587. [[CrossRef](#)]
2. Ranga, C.; Kumar, A.; Chandel, R. Influence of electrical and thermal ageing on the mineral insulating oil performance for power transformer applications. *Insight-Non-Destr. Test. Cond. Monit.* **2020**, *62*, 222–231. [[CrossRef](#)]
3. Li, L.; Song, J.; Lei, Z.; Kang, A.; Wang, Z.; Men, R.; Ma, Y. Effects of ambient humidity and thermal aging on properties of Nomex insulation in mining dry-type transformer. *High Volt.* **2021**, *6*, 71–81. [[CrossRef](#)]
4. Wei, X.; Xiong, J.; Wang, J.; Xu, W. New advances in fiber-reinforced composite honeycomb materials. *Sci. China Technol. Sci.* **2020**, *63*, 1348–1370. [[CrossRef](#)]
5. Gao, Y.; Chen, X.; Wei, Y. Graded honeycombs with high impact resistance through machine learning-based optimization. *Thin-Walled Struct.* **2023**, *188*, 110794. [[CrossRef](#)]
6. Xie, S.; Wang, H.; Jing, K.; Feng, Z. Mechanical properties of Nomex honeycombs filled with tubes of carbon fiber reinforced vinyl ester resin composites. *Thin-Walled Struct.* **2022**, *180*, 109933. [[CrossRef](#)]
7. Zarrouk, T.; Nouari, M.; Makich, H. Simulated study of the machinability of the Nomex honeycomb structure. *J. Manuf. Mater. Process.* **2023**, *7*, 28. [[CrossRef](#)]
8. Jaafar, M.; Atlati, S.; Makich, H.; Nouari, M.; Moufki, A.; Julliere, B. A 3D FE modeling of machining process of Nomex[®] honeycomb core: Influence of the cell structure behavior and specific tool geometry. *Procedia Cirp* **2017**, *58*, 505–510. [[CrossRef](#)]
9. Dong, Z.; Qin, Y.; Kang, R.; Wang, Y.; Sun, J.; Zhu, X.; Liu, Y. Robust cell wall recognition of laser measured honeycomb cores based on corner type identification. *Opt. Lasers Eng.* **2021**, *136*, 106321. [[CrossRef](#)]
10. Jaafar, M.; Makich, H.; Nouari, M. A new criterion to evaluate the machined surface quality of the Nomex[®] honeycomb materials. *J. Manuf. Process.* **2021**, *69*, 567–582. [[CrossRef](#)]
11. Xie, W.; Wang, X.; Liu, E.; Wang, J.; Tang, X.; Li, G.; Zhao, B. Research on cutting force and surface integrity of TC18 titanium alloy by longitudinal ultrasonic vibration assisted milling. *Int. J. Adv. Manuf. Technol.* **2022**, *119*, 4745–4755. [[CrossRef](#)]
12. Sun, J.; Kang, R.; Qin, Y.; Wang, Y.; Feng, B.; Dong, Z. Simulated and experimental study on the ultrasonic cutting mechanism of aluminum honeycomb by disc cutter. *Compos. Struct.* **2021**, *275*, 114431. [[CrossRef](#)]
13. Xia, Y.; Zhang, J.; Wu, Z.; Feng, P.; Yu, D. Study on the design of cutting disc in ultrasonic assisted machining of honeycomb composites. *IOP Conf. Ser. Mater. Sci. Eng.* **2019**, *611*, 012032. [[CrossRef](#)]
14. Sun, J.; Dong, Z.; Wang, X.; Wang, Y.; Qin, Y.; Kang, R. Simulation and experimental study of ultrasonic cutting for aluminum honeycomb by disc cutter. *Ultrasonics* **2020**, *103*, 106102. [[CrossRef](#)] [[PubMed](#)]
15. Ahmad, S.; Zhang, J.; Feng, P.; Yu, D.; Wu, Z.; Ke, M. Research on design and FE simulations of novel ultrasonic circular saw blade (UCSB) cutting tools for rotary ultrasonic machining of Nomex honeycomb composites. In Proceedings of the 2019 16th International Bhurban Conference on Applied Sciences and Technology (IBCAST), Islamabad, Pakistan, 8–12 January 2019; pp. 113–119.
16. Kang, D.; Zou, P.; Wu, H.; Duan, J.; Wang, W. Study on ultrasonic vibration-assisted cutting of Nomex honeycomb cores. *Int. J. Adv. Manuf. Technol.* **2019**, *104*, 979–992. [[CrossRef](#)]
17. Xiang, D.H.; Wu, B.F.; Yao, Y.L.; Liu, Z.Y.; Feng, H.R. Ultrasonic longitudinal-torsional vibration-assisted cutting of Nomex (R) honeycomb-core composites. *Int. J. Adv. Manuf. Technol.* **2019**, *100*, 1521–1530. [[CrossRef](#)]
18. Wojciechowski, S.; Matuszak, M.; Powalka, B.; Madajewski, M.; Maruda, R.W.; Krolczyk, G.M. Prediction of cutting forces during micro end milling considering chip thickness accumulation. *Int. J. Mach. Tools Manuf.* **2019**, *147*, 103466. [[CrossRef](#)]
19. Yuan, Y.J.; Jing, X.B.; Ehmann, K.F.; Cao, J.; Li, H.Z.; Zhang, D.W. Modeling of cutting forces in micro end-milling. *J. Manuf. Process.* **2018**, *31*, 844–858. [[CrossRef](#)]
20. Ahmad, S.; Zhang, J.; Feng, P.; Yu, D.; Wu, Z. Experimental study on rotary ultrasonic machining (RUM) characteristics of Nomex honeycomb composites (NHCs) by circular knife cutting tools. *J. Manuf. Process.* **2020**, *58*, 524–535. [[CrossRef](#)]
21. Zarrouk, T.; Nouari, M.; Salhi, J.E.; Benbouaza, A. Numerical Simulation of Rotary Ultrasonic Machining of the Nomex Honeycomb Composite Structure. *Machines* **2024**, *12*, 137. [[CrossRef](#)]
22. Foo, C.C.; Chai, G.B.; Seah, L.K. Mechanical properties of Nomex material and Nomex honeycomb structure. *Compos. Struct.* **2007**, *80*, 588–594. [[CrossRef](#)]
23. Roy, R.; Park, S.J.; Kweon, J.H.; Choi, J.H. Characterization of Nomex honeycomb core constituent material mechanical properties. *Compos. Struct.* **2014**, *117*, 255–266. [[CrossRef](#)]

24. Nasir, M.A.; Khan, Z.; Farooqi, I.; Nauman, S.; Anas, S.; Khalil, S.; Ata, R. Transverse shear behavior of a Nomex core for sandwich panels. *Mech. Compos. Mater.* **2015**, *50*, 733–738. [[CrossRef](#)]
25. Arnold, G.; Leiteritz, L.; Zahn, S.; Rohm, H. Ultrasonic cutting of cheese: Composition affects cutting work reduction and energy demand. *Int. Dairy J.* **2009**, *19*, 314–320. [[CrossRef](#)]

Disclaimer/Publisher’s Note: The statements, opinions and data contained in all publications are solely those of the individual author(s) and contributor(s) and not of MDPI and/or the editor(s). MDPI and/or the editor(s) disclaim responsibility for any injury to people or property resulting from any ideas, methods, instructions or products referred to in the content.